Contrast Ultrasound Imaging Does Not Affect Heat Shock Protein 70 Expression in Cholesterol-Fed Rabbit Aorta

Brendon W. Smith, PhD, Douglas G. Simpson, PhD, Rita J. Miller, DVM, John W. Erdman Jr, PhD, William D. O'Brien Jr, PhD

Objectives—Diagnostic ultrasound imaging is enhanced by the use of circulating microbubble contrast agents (UCAs), but the interactions between ultrasound, UCAs, and vascular tissue are not fully understood. We hypothesized that ultrasound with a UCA would stress the vascular tissue and increase levels of heat shock protein 70 (Hsp70), a cellular stress protein.

Methods—Male New Zealand White rabbits (n = 32) were fed a standard chow diet (n = 4) or a 1% cholesterol, 10% fat, and 0.11% magnesium diet (n = 28). At 21 days, 24 rabbits on the cholesterol diet were either exposed to ultrasound (3.2-MHz f/3 transducer; 2.1 MPa; mechanical index, 1.17; 10 Hz pulse repetition frequency; 1.6 microseconds pulse duration; 2 minutes exposure duration at 4 sites along the aorta) with the UCA Definity (1× concentration, 1 mL/min; Lantheus Medical Imaging, North Billerica, MA) or sham exposed with a saline vehicle injection (n = 12 per group). Four rabbits on the cholesterol diet and 4 on the chow diet served as cage controls and were not exposed to ultrasound or restrained for blood sample collection. Animals were euthanized 24 hours after exposure, and aortas were quickly isolated and frozen in liquid nitrogen. Aorta lysates from the area of ultrasound exposure were analyzed for Hsp70 level by Western blot. Blood plasma was analyzed for cholesterol, Hsp70, and von Willebrand factor, a marker of endothelial function.

Results—Plasma total cholesterol levels increased to an average of 705 mg/dL. Ultrasound did not affect plasma von Willebrand factor, plasma Hsp70, or aorta Hsp70. Restraint increased Hsp70 ($P < .001$, analysis of variance).

Conclusions—Restraint, but not ultrasound with the UCA or cholesterol feeding, significantly increased Hsp70.

Key Words—atherosclerosis; cardiovascular disease; contrast agents; endothelium; heat shock protein 70; microbubbles; ultrasound

Received May 16, 2014, from the Bioacoustics Research Laboratory, Department of Electrical and Computer Engineering (B.W.S., R.J.M., W.D.O.), Division of Nutritional Sciences (B.W.S., J.W.E., W.D.O.), and Departments of Statistics (D.G.S.) and Food Science and Human Nutrition (J.W.E.), University of Illinois at Urbana-Champaign, Urbana, Illinois USA. Revision requested July 12, 2014. Revised manuscript accepted for publication October 24, 2014.

We thank Rami Abuhabsah, Jim Blue, Michael Kurowski, Matt Lee, Sandhya Sarwate, MD, and Presence Covenant Medical Center for their contributions. This work was supported by National Institutes of Health grant R37EB002641.

Address correspondence to William D. O'Brien Jr, PhD, Bioacoustics Research Laboratory, Department of Electrical and Computer Engineering, University of Illinois at Urbana-Champaign, 405 N Mathews Ave, Urbana, IL 61801 USA.

E-mail: wdo@uiuc.edu

Abbreviations

CV, coefficient of variation; ELISA, enzyme-linked immunosorbent assay; HDL, high-density lipoprotein; Hsp70, heat shock protein 70; LDL, low-density lipoprotein; UCA, ultrasound contrast agent; vWF, von Willebrand factor

doi:10.7863/ultra.34.7.1209

Cardiovascular disease remains the leading cause of death in the United States and worldwide.[1] Atherosclerosis, the deposition and development of lipid-rich arterial plaques, is the pathogenic process underlying most cardiovascular events.[2,3] Evidence suggests atherosclerosis is reversible in its early stages,[4] but it develops asymptomatically and is frequently undetected until it results in heart attacks and strokes. Early detection is thus a critical frontier in reducing deaths from cardiovascular disease. Ultrasound imaging is a flexible, inexpensive, widely used, and real-time imaging modality that can be used for early detection and diagnosis of

cardiovascular disease.[5–8] Diagnostic ultrasound imaging is improved by the use of microbubble ultrasound contrast agents (UCAs), which are injected intravenously before imaging. The interaction of ultrasound with UCAs in the circulation causes them to oscillate or collapse and aids in delineation of tissue. In some cardiac imaging situations, ultrasound alone is unable to provide a clear image, but the addition of UCAs can improve images to diagnostic quality.[9]

Although the clinical benefits of UCAs are established, the effects of the ultrasound-UCA interaction on cardiac and arterial tissue are not well understood. Contrast ultrasound imaging of the cardiovascular system is not typically performed in asymptomatic patients without risk factors. Rather, most patients will have some degree of disease present.[10] Rabbits were fed a cholesterol diet to reflect this scenario, increasing the translational relevance of the model.

We performed contrast ultrasound imaging of the aorta on cholesterol-fed rabbits and hypothesized that the interaction of ultrasound with UCAs in the blood would stress the vascular tissue and increase levels of heat shock protein 70 (Hsp70), a cellular stress protein.

Materials and Methods

Animals and Experimental Design

The University of Illinois Institutional Animal Care and Use Committee approved all live animal procedures. Twenty-eight male New Zealand White rabbits (Myrtle's Rabbitry, Thompson's Station, TN; and Covance, Princeton, NJ) consumed a 1% cholesterol, 10% fat, and 0.11% magnesium diet (5TZB; TestDiet, Richmond, IN) for 3 weeks as previously described[11] (Figure 1). An additional 4 rabbits consumed a chow diet (2031 Global High-Fiber Rabbit Diet; Harlan Teklad, Madison, WI) throughout the study. Animals were provided 140 g/d of feed. After 3 weeks, 24 animals on the cholesterol diet were randomized to receive either an ultrasound exposure at 2.1 MPa with the UCA Definity (Lantheus Medical Imaging, North Billerica, MA; n = 12) or a sham exposure with the saline UCA vehicle (n = 12). Blood samples were obtained from the lateral saphenous vein weekly, as well as 1 hour before, 1 hour after, and 24 hours after ultrasound exposure. Animals were then euthanized 24 hours after ultrasound exposure to allow adequate time for induction of Hsp70.[12,13] Aorta tissue from the site of ultrasound exposure (5 mm length, 10–20 mg) was rapidly isolated, rinsed with cold phosphate-buffered saline to remove blood, frozen in liquid nitrogen, and stored at –50°C.

Exposimetry

The ultrasound procedures have been previously described in considerable detail using a calibrated polyvinylidene fluoride membrane hydrophone (Y-34–3598 EW295; GEC Marconi, Chelmsford, England) with a 0.5-mm-diameter active element.[11,14] Ultrasound exposures were performed using a 3.2-MHz f/3, 19-mm-diameter lithium niobate single-element transducer (4 exposure sites, 2 minutes per exposure as previously described[11]) with intravenous infusion of Definity (2.6% Definity in saline, 1 mL/min, 15–20 minutes total infusion time). A separate ultrasound system was used to guide and position the single-element transducer for exposures (Ultrasonix Medical Corporation, Richmond, British Columbia, Canada). The transducer was regularly calibrated in degassed water. To account for in vivo attenuation of the ultrasound signal, we also calculated the attenuation slope and in situ derated peak rarefactional pressure amplitude using the radiofrequency data set. The in situ peak rarefactional pressure amplitude in this study was 2.1 MPa, corresponding to a mechanical index of 1.17, with a 10 Hz pulse repetition frequency, 1.6 microsecond pulse duration, and 2 minute exposure duration at each of 4 sites along the abdominal aorta (exposure 1, 2 mm cranial to the cranial edge of the renal artery; exposure 2, 2 mm caudal to exposure 1; exposure 3, 2 mm caudal to exposure 2; exposure 4, 2 mm caudal to exposure 3).

Figure 1. Study design with 32 New Zealand White (NZW) rabbits. After 3 weeks on either the chow diet or the 1% cholesterol, 10% fat, and 0.11% magnesium diet, rabbits (n = 24) underwent ultrasound (US) imaging at 2.1 MPa with intravenous administration of the Definity UCA or a sham procedure. Serial saphenous vein blood samples were collected from these animals under restraint. An additional 4 rabbits on the cholesterol diet and the 4 on chow served as cage controls. Rabbits were euthanized 24 hours after the ultrasound procedure (day 22), and aorta tissue was collected for analysis.

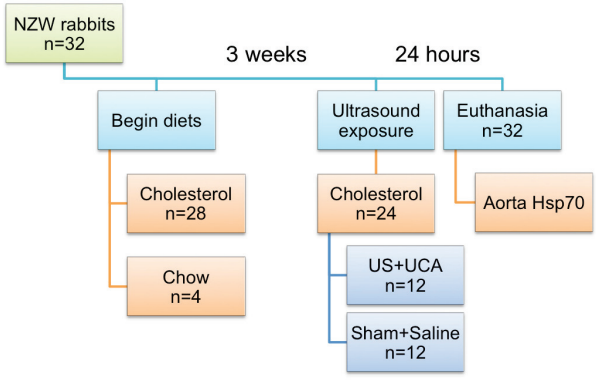

Western Blotting

Aorta tissue was homogenized in 4°C radioimmunoprecipitation assay buffer with a protease inhibitor mixture (Sigma-Aldrich, St Louis, MO) using a glass tissue grinder (Pyrex; Corning, Tewksbury, MA) followed by a handheld motorized homogenizer (Polytron PT1200E; Kinematica, Inc, Bohemia, NY). Lysates were kept on ice with agitation for 30 minutes, centrifuged for 10 minutes at 10,000g and 4°C, aliquoted, and frozen at −50°C. Protein concentrations were determined in triplicate with a Bradford assay (Bio-Rad, Hercules, CA). Lysates were then diluted 1:1 in Laemmli sample buffer with 5% β-mercaptoethanol (Bio-Rad), heated at 95°C for 5 minutes, and centrifuged at 3000g for 1 minute. Equal amounts of total protein (20 μg per sample) were loaded onto 10% Tris-glycine gels (Mini-Protean TGX; Bio-Rad), and electrophoresis was performed for 35 minutes at 200 V (Mini-Protean Tetra Cell with PowerPac HC power supply; Bio-Rad). Proteins were then transferred onto nitrocellulose membranes with a semidry transfer cell (Bio-Rad) for 30 minutes at 15 V. Total protein transfer was verified by staining with 0.1% Ponceau S (Sigma-Aldrich) for 5 minutes, and the stain was then removed by washing membranes in 0.1 M sodium hydroxide for 30 seconds, followed by a brief rinse in deionized water. Western blotting was performed with the Fast Western kit (Pierce Biotechnology, Rockford, IL) according to the manufacturer's instructions, using a mouse monoclonal anti-Hsp70 antibody (clone C92F3A-5; Enzo Life Sciences, Inc, Farmingdale, NY) with mouse monoclonal anti-β-actin (clone AC-15; Novus Biologicals, Littleton, CO) as a loading control. Purified Hsp70 and heat shock cognate protein 70 (Enzo) were included as positive and negative controls, respectively. Membranes were imaged using a ChemiDoc XRS system with Quantity One software (Bio-Rad). Data are expressed as density of the Hsp70 band divided by density of the β-actin band after local background subtraction.

Blood Analysis

Plasma total cholesterol, low-density lipoprotein (LDL), high-density lipoprotein (HDL), and triglyceride levels were determined in triplicate using enzymatic colorimetric kits (Wako Chemicals, Richmond, VA) with human control sera (Wako) included in each assay to evaluate precision. A coefficient of variation (CV) was used as a measure of precision. The intra-assay CVs for control sera were 5.0% for total cholesterol, 8.1% for LDL, 5.3% for HDL, and 6.6% for triglycerides. The inter-assay CVs for control sera were 8.2% for total cholesterol, 8.0% for LDL, 23% for HDL, and 16% for triglycerides. The intra-assay CVs for rabbit plasma samples were 4.1% for total cholesterol, 5.7% for LDL, 3.7% for HDL, and 4.5% for triglycerides. Measurement of plasma von Willebrand factor (vWF) was performed by an enzyme-linked immunosorbent assay (ELISA) as previously described.[15] The intra-assay CV for rabbit plasma vWF was 2.3%. Plasma Hsp70 was measured in duplicate by ELISA (Enzo) according to the manufacturer's instructions. The average intra-assay CV for the Hsp70 ELISA was 2.7%, and the average inter-assay CV was 42%.

Statistical Analysis

Feed intakes, body weights, blood cholesterol, and Hsp70 data were evaluated with an analysis of variance or analysis of covariance approach in the general linear mixed models procedure of SAS 9.3 (SAS Institute Inc, Cary, NC) as previously described.[16] Plasma and aorta Hsp70 were also evaluated for correlation using simple linear regression in SAS. von Willebrand factor were analyzed in R (www.r-project.org) as previously described.[11] Repeated measures analyses incorporated baseline values as a covariate random effect when the term contributed significantly to the statistical model. Data sets that did not meet the assumption of normality (Shapiro-Wilk $W < 0.9$ or Spearman rank order correlation $P < .05$) were log transformed. Bonferroni adjustments for multiple comparisons were made when necessary, and statistical significance was declared at $P < .05$.

Results

Feed Intake and Body Weights

Chow-fed animals consumed all 140 g/d they were provided throughout the study. Feed intake decreased significantly over time in cholesterol diet groups. By week 3, feed intake decreased significantly in cholesterol-fed animals to 88 g/d compared with 140 g/day for those fed chow ($P < .05$). Body weights averaged 3.0 kg at baseline and 3.3 kg after 3 weeks and did not differ among diet groups ($P = .16$, adjusted for baseline body weight). Ultrasound did not affect feed intake ($P = .35$) or body weight ($P = .97$).

Contrast Ultrasound Does Not Affect Circulating Cholesterol or vWF

Plasma total cholesterol initially averaged 25 mg/dL and quickly escalated after introduction of the cholesterol diet, reaching an average of 705 mg/dL by the end of the study ($P < .0001$; Figure 2A). No difference in plasma cholesterol levels was observed between animals receiving ultrasound with the UCA and animals receiving the sham

treatment (P = .57). Plasma LDL increased in parallel with total cholesterol, reaching 468 mg/dL after 3 weeks. Low-density lipoprotein decreased after the experimental procedure at 3 weeks in both sham and ultrasound-exposed animals (P < .001), and returned to pretreatment levels 24 hours later. High-density lipoprotein levels remained unchanged throughout the study, and averaged 41 mg/dL. Plasma triglyceride levels increased from 37.2 to 130 mg/dL after consumption of the cholesterol diet (P < .0001), but were not altered by the ultrasound procedure. Plasma vWF levels also increased from 166 to 2840 mg/dL during cholesterol feeding, but did not change significantly 1 hour (P = .72) or 24 hours (P = .27) after ultrasound compared with animals receiving the sham treatment (Figure 2B).

Contrast Ultrasound Does Not Affect Aorta or Plasma Hsp70 Levels

Rabbits that had been restrained for serial blood sample collection had significantly higher aorta Hsp70 than control rabbits that had not been restrained, regardless of diet (P < .001; Figure 3). Ultrasound with the UCA did not significantly affect aorta Hsp70 levels. Plasma Hsp70 was significantly lower at 22 days than before experimental procedures on day 21, regardless of ultrasound treatment group (P < .01; Figure 4A), but was otherwise not significantly altered throughout the study. No correlation was observed between tissue and plasma Hsp70 levels 24 hours after ultrasound exposure ($F_{(1,9)}$ = 0.9; r^2 = 0.083; P = .36 for sham + saline; $F_{(1,9)}$ = 0.04; r^2 = 0.005; P = .84 for ultrasound + UCA; Figure 4B). One animal had plasma Hsp70 levels an average of 10 SDs above the mean throughout the study (including at baseline), and was therefore excluded from the data set during analysis.

Discussion

When exposed to ultrasound, microbubbles dynamically expand and contract[17] in response to the temporal varying acoustic pressure amplitude. Ultrasound induces oscillation of UCAs at lower pressure levels and collapse at higher pressures. The biophysical interaction of ultrasound with circulating microbubbles increases the echogenicity of blood and results in improved contrast between blood and tissue. For this reason, UCAs have proven useful in enhancement of clinical ultrasound images. The ultrasound-UCA interaction is useful for imaging, but may cause other biological effects. Although clinical trials and meta-analyses have recently dispelled concerns over the safety of UCAs in human patients,[18–23] there is a large body of experimental research literature that has not been controverted. Ultrasound and UCAs have induced capillary rupture and hemorrhage,[24–26] cardiac damage,[27] and arrhythmias[28] and impaired vascular endothelial function[29] in animal studies. Ultrasound has been shown to mechanically disturb cell membranes, inducing temporary permeability in a phenomenon known as sonoporation.[30–35] Microbubble UCAs are used in cardiovascular imaging, so it is important to evaluate their effects on the heart and blood vessels. We hypothesized that the interaction of ultrasound with UCAs would stress the vasculature at the site of ultrasound exposure, resulting in increased levels of the stress protein Hsp70.

Figure 2. Plasma cholesterol and vWF. **A**, Plasma total cholesterol (TC) was measured by an enzymatic colorimetric kit. **B**, Plasma vWF was measured by ELISA. TG indicates triglycerides.

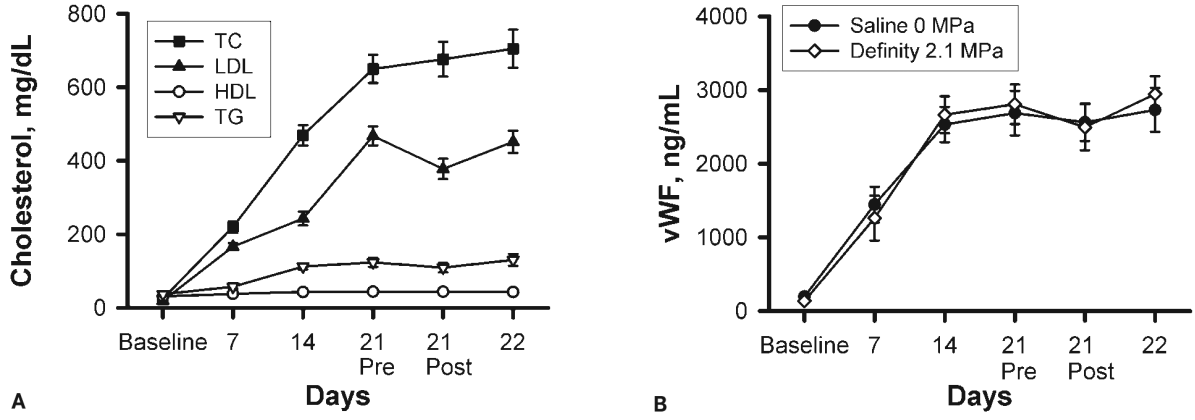

Fundamentally, proteins are chains of amino acids joined by peptide bonds. These amino acid chains (primary structures) must fold into specific 3-dimensional conformations (tertiary structures) to achieve their catalytic activity. A protein's tertiary structure is determined by its primary amino acid sequence in vitro,[36] but in the complex in vivo cellular environment, proteins require assistance from a quality control system of molecular chaperones to ensure proper folding.[37] These chaperones mediate not only proper initial folding of proteins but also refolding during times of cellular stress, including oxidative stress, exposure to ethanol and other toxins, pH or osmotic changes, ultraviolet radiation, and elevated temperatures.[37,38] All living organisms respond to elevated temperatures and other forms of cellular stress by producing a class of chaperones known as heat shock proteins,[39] with Hsp70 being one of the most robustly produced in times of cellular stress. The induction of heat shock proteins is primarily controlled at the translational level.[40–42] For this reason, we chose to measure protein levels of Hsp70 instead of messenger RNA. Translated heat shock protein products appear within minutes of heat shock in cultured cells.[43] The reported half-life of Hsp70 varies by model system and experimental conditions,[44–49] but was recently estimated to be 18 hours by quantitative proteomic profiling of U937 cells after heat shock.[50] Although Hsp70 has been detected within minutes in cell culture studies, measurable induction of the heat shock response takes longer in a physiologic context. We selected our euthanasia time point of 24 hours after ultrasound to allow for induction of Hsp70 expression in rabbit aorta.[12,13]

Hsp70, and several other heat shock proteins, are involved in the cardiovascular system and cardiovascular disease.[51] Cells in the heart and blood vessels respond to stress by increasing production of Hsp70. Intracellular Hsp27, 70, and 90 protect against the stresses of atherosclerosis, but circulating soluble Hsp60 can activate both the innate and adaptive immune systems.[52,53] Heat shock increases the ability to withstand subsequent heat shock and environmental stress. As evidence of this thermotolerance, prior heat shock reduces myocardial infarct size in animal

Figure 3. Aorta tissue Hsp70 analysis on day 22. Aorta tissue from the site of exposure was carefully dissected from the surrounding tissue and frozen in liquid nitrogen. Tissue lysates were analyzed for Hsp70 by Western blot, with β-actin as a loading control. Western blot bands shown are representative of the mean of each group. Bars indicate SEM; + and – indicate presence and absence of the treatment.

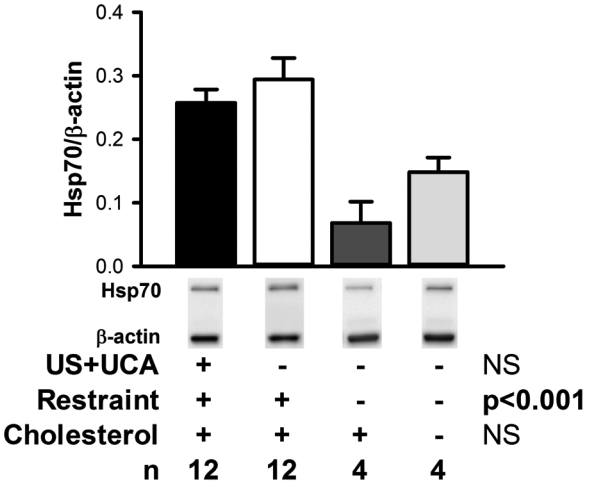

Figure 4. Plasma Hsp70. **A**, Plasma Hsp70 was measured by ELISA. **B**, There was no correlation between plasma and tissue Hsp70 levels. Bars indicate SEM.

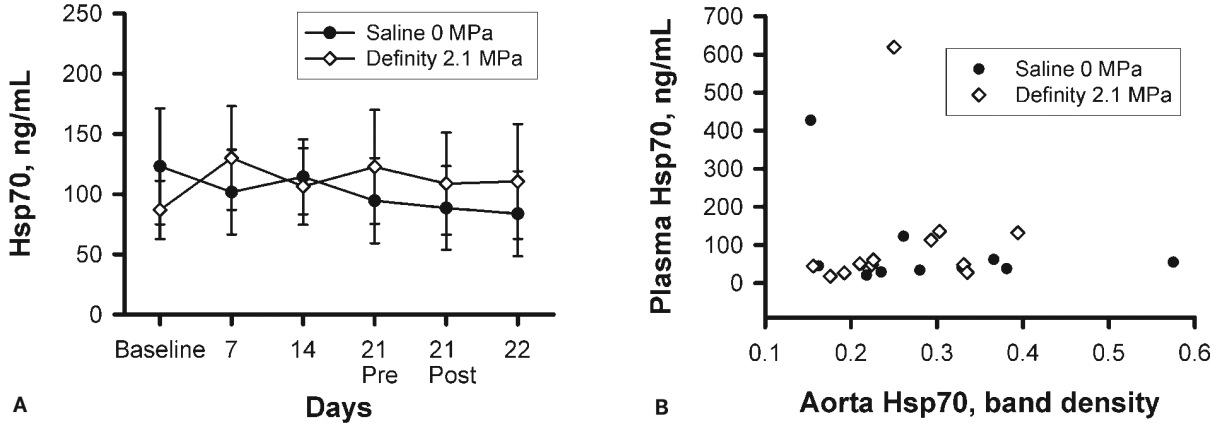

models.[12,54,55] Thermotolerance is most effectively induced when the animals are heat shocked 24 hours before infarction, providing further support for our selection of euthanasia time. Mechanical stress is another activator of the heat shock response, and the studies of sonoporation referenced above have demonstrated ultrasound-induced mechanical effects on cell membranes, providing an additional rationale for the inclusion of Hsp70 as a cellular stress marker.

Several other studies have evaluated the effects of ultrasound on heat shock proteins. Hsp70 and other heat shock proteins have been used as biomarkers in studies of high-intensity focused ultrasound, an application that is emerging as a potential treatment for cancer. High-intensity focused ultrasound technology delivers concentrated ultrasonic energy to tumors, causing an elevation in temperature sufficient to kill the tumor cells while leaving surrounding tissue intact. Studies of cultured cancer cells,[56] mice,[57,58] and human patients with breast cancer[59] have demonstrated increases in Hsp60 and Hsp70 after high-intensity focused ultrasound. It is important to note that high-intensity focused ultrasound uses ultrasound exposure conditions that are more intense than clinical contrast ultrasound exposures. It is important to investigate ultrasound parameters beyond those used in the clinic to set safety thresholds. However, they are not clinically relevant in the sense that a patient would not experience this amount of ultrasonic energy deposition during cardiovascular contrast ultrasound imaging. Although our mechanical index of 1.17 is above the manufacturer's recommendation of 0.8 for use with Definity, it is closer to a realistic scenario. The ultrasound exposure conditions used in this study, and those used in clinical contrast ultrasound imaging, do not induce appreciable heating of tissue,[60] but may result in other nonthermal biological effects as described above. Another study used contrast ultrasound to monitor radiofrequency thermal ablation of rabbit liver tissue.[61] The authors noted a qualitative increase in Hsp70 expression after radiofrequency ablation and, interestingly, also a modest increase in Hsp70 with contrast ultrasound alone. This study used a different UCA, Sonazoid (GE Healthcare, Princeton, NJ), with a similar phospholipid shell composition as Definity, at an unknown concentration in a bolus infusion. The authors posited that this biological effect was due to the interaction of ultrasound with UCAs. There is not currently strong evidence that biological effects will vary as a function of UCA type, but the potential does exist, as lipid-shelled microbubbles exhibit different biophysical properties than albumin-shelled microbubbles when interacting with ultrasound.[62,63]

The effect of ultrasound on Hsp70 has also been investigated in rat muscle. Although acute ultrasound exposure did not induce Hsp70,[64] a series of 4 exposures did result in increased production of Hsp70.[65] These two studies used a 1-MHz transducer without a UCA and measured Hsp70 by Western blot using an antibody similar to the one used in our study. The rabbit and rat studies described above also chose a 24-hour postexposure time point for collection of tissue samples. Importantly, none of these studies have focused on the cardiovascular system, the primary target of contrast ultrasound imaging, using clinically relevant contrast ultrasound exposure conditions. The biological effects of contrast ultrasound may vary by tissue. For example, the lungs are particularly susceptible to damage by ultrasound and UCAs.[66,67] The vasculature is also susceptible to damage, but it is not yet clear whether it is more or less susceptible than other tissues. The lack of an effect seen in this work suggests that the ultrasound pressure levels and UCA concentrations used clinically are below the threshold for tissue damage and induction of Hsp70.

Blood collection from the lateral saphenous vein requires restraint of the animals. We included unrestrained control groups of cholesterol- and chow-fed animals to account for the effect of restraint and found that restrained animals had significantly higher aorta Hsp70 levels, regardless of diet (Figure 3). Previous work has shown that restraint stress can induce aorta Hsp70 expression in rats,[68] and we have now demonstrated this effect in rabbits. However, we cannot rule out the possibility that anesthetics may have contributed to the elevated Hsp70 levels seen in these rabbits. Anesthesia has been shown to increase Hsp70 levels in rats.[69] We also observed a decrease in LDL after the experimental procedure at 3 weeks, independent of ultrasound treatment. Anesthetics have been shown to affect blood cholesterol levels,[70,71] and it is possible that the LDL fraction was particularly affected. In addition to plasma lipids and Hsp70, we also measured plasma vWF (Figure 2B). von Willebrand factor is a clotting protein produced and secreted by endothelial cells, and it serves as a marker of endothelial function.[72,73] We included vWF to identify any acute effects of contrast ultrasound on the vascular endothelium. The lack of an effect of imaging on vWF suggests that the endothelium was not disturbed by the procedure.

In conclusion, we have conducted an assessment of contrast ultrasound imaging focused on vascular stress, with aorta Hsp70 levels as the key indicator. Hsp70 was expressed in vascular tissue, but no additional vascular stress was observed as a result of the imaging procedures.

References

1. Go AS, Mozaffarian D, Roger VL, et al. Heart disease and stroke statistics—2013 update: a report from the American Heart Association. *Circulation* 2013; 127:e6–e245.
2. Hansson GK, Hermansson A. The immune system in atherosclerosis. *Nat Immunol* 2011; 12:204–212.
3. Libby P, Ridker PM, Hansson GK. Progress and challenges in translating the biology of atherosclerosis. *Nature* 2011; 473:317–325.
4. Tabas I, Williams KJ, Borén J. Subendothelial lipoprotein retention as the initiating process in atherosclerosis: update and therapeutic implications. *Circulation* 2007; 116:1832–1844.
5. Greenland P, Alpert JS, Beller GA, et al. 2010 ACCF/AHA guideline for assessment of cardiovascular risk in asymptomatic adults: a report of the American College of Cardiology Foundation/American Heart Association Task Force on Practice Guidelines. *Circulation* 2010; 122:e584–e636.
6. Fuster V, Lois F, Franco M. Early identification of atherosclerotic disease by noninvasive imaging. *Nat Rev Cardiol* 2010; 7:327–333.
7. Coller JM, Campbell DJ, Krum H, Prior DL. Early identification of asymptomatic subjects at increased risk of heart failure and cardiovascular events: progress and future directions. *Heart Lung Circ* 2013; 22:171–178.
8. Cote AT, Harris KC, Panagiotopoulos C, Sandor GGS, Devlin AM. Childhood obesity and cardiovascular dysfunction. *J Am Coll Cardiol* 2013; 62:1309–1319.
9. Reilly JP, Tunick PA, Timmermans RJ, Stein B, Rosenzweig BP, Kronzon I. Contrast echocardiography clarifies uninterpretable wall motion in intensive care unit patients. *J Am Coll Cardiol* 2000; 35:485–490.
10. Mulvagh SL, Rakowski H, Vannan MA, et al. American Society of Echocardiography Consensus Statement on the Clinical Applications of Ultrasonic Contrast Agents in Echocardiography. *J Am Soc Echocardiogr* 2008; 21:1179–1201.
11. Smith BW, Simpson DG, Sarwate S, et al. Contrast ultrasound imaging of the aorta alters vascular morphology and circulating von Willebrand factor in hypercholesterolemic rabbits. *J Ultrasound Med* 2012; 31:711–720.
12. Marber MS, Latchman DS, Walker JM, Yellon DM. Cardiac stress protein elevation 24 hours after brief ischemia or heat stress is associated with resistance to myocardial infarction. *Circulation* 1993; 88:1264–1272.
13. Hauser GJ, Dayao EK, Wasserloos K, Pitt BR, Wong HR. HSP induction inhibits iNOS mRNA expression and attenuates hypotension in endotoxin-challenged rats. *Am J Physiol* 1996; 271:H2529–H2535.
14. Zachary JF, Frizzell LA, Norrell KS, Blue JP Jr, Miller RJ, O'Brien WD Jr. Temporal and spatial evaluation of lesion reparative responses following superthreshold exposure of rat lung to pulsed ultrasound. *Ultrasound Med Biol* 2001; 27:829–839.
15. Smith BW, Strakova J, King JL, Erdman JW Jr, O'Brien WD Jr. Validated sandwich ELISA for the quantification of von Willebrand factor in rabbit plasma. *Biomark Insights* 2010; 5:119–127.
16. Smith BW, King JL, Miller RJ, et al. Optimization of a low magnesium, cholesterol-containing diet for the development of atherosclerosis in rabbits. *J Food Res* 2013; 2:168–178.
17. King DA, O'Brien WD Jr. Comparison between maximum radial expansion of ultrasound contrast agents and experimental postexcitation signal results. *J Acoust Soc Am* 2011; 129:114–121.
18. Herzog CA. Incidence of adverse events associated with use of perflutren contrast agents for echocardiography. *JAMA* 2008; 299:2023–2025.
19. Wei K, Mulvagh SL, Carson L, et al. The safety of Definity and Optison for ultrasound image enhancement: a retrospective analysis of 78,383 administered contrast doses. *J Am Soc Echocardiogr* 2008; 21:1202–1206.
20. Dolan MS, Gala SS, Dodla S, et al. Safety and efficacy of commercially available ultrasound contrast agents for rest and stress echocardiography: a multicenter experience. *J Am Coll Cardiol* 2009; 53:32–38.
21. Main ML. Ultrasound contrast agent safety: from anecdote to evidence. *JACC Cardiovasc Imaging* 2009; 2:1057–1059.
22. Abdelmoneim SS, Bernier M, Scott CG, et al. Safety of contrast agent use during stress echocardiography in patients with elevated right ventricular systolic pressure: a cohort study. *Circ Cardiovasc Imaging* 2010; 3:240–248.
23. Khawaja OA, Shaikh KA, Al-Mallah MH. Meta-analysis of adverse cardiovascular events associated with echocardiographic contrast agents. *Am J Cardiol* 2010; 106:742–747.
24. Miller DL, Quddus J. Diagnostic ultrasound activation of contrast agent gas bodies induces capillary rupture in mice. *Proc Natl Acad Sci USA* 2000; 97:10179–10184.
25. Miller DL. Induction of pulmonary hemorrhage in rats during diagnostic ultrasound. *Ultrasound Med Biol* 2012; 38:1476–1482.
26. Miller DL, Dou C, Sorenson D, Liu M. Histological observation of islet hemorrhage induced by diagnostic ultrasound with contrast agent in rat pancreas. *PloS One* 2011; 6:e21617.
27. Miller DL, Li P, Gordon D, Armstrong WF. Histological characterization of microlesions induced by myocardial contrast echocardiography. *Echocardiography* 2005; 22:25–34.
28. Zachary JF, Hartleben SA, Frizzell LA, O'Brien WD Jr. Arrhythmias in rat hearts exposed to pulsed ultrasound after intravenous injection of a contrast agent. *J Ultrasound Med* 2002; 21:1347–1356.
29. Wood SC, Antony S, Brown RP, et al. Effects of ultrasound and ultrasound contrast agent on vascular tissue. *Cardiovasc Ultrasound* 2012; 10:29.
30. Bao S, Thrall BD, Miller DL. Transfection of a reporter plasmid into cultured cells by sonoporation in vitro. *Ultrasound Med Biol* 1997; 23:953–959.
31. Tachibana K, Uchida T, Ogawa K, Yamashita N, Tamura K. Induction of cell-membrane porosity by ultrasound. *Lancet* 1999; 353:1409.
32. Miller DL, Quddus J. Sonoporation of monolayer cells by diagnostic ultrasound activation of contrast-agent gas bodies. *Ultrasound Med Biol* 2000; 26:661–667.
33. Marmottant P, Hilgenfeldt S. Controlled vesicle deformation and lysis by single oscillating bubbles. *Nature* 2003; 423:153–156.
34. Deng CX, Sieling F, Pan H, Cui J. Ultrasound-induced cell membrane porosity. *Ultrasound Med Biol* 2004; 30:519–526.
35. Forbes MM, Steinberg RL, O'Brien WD Jr. Examination of inertial cavitation of Optison in producing sonoporation of Chinese hamster ovary cells. *Ultrasound Med Biol* 2008; 34:2009–2018.
36. Anfinsen CB. Principles that govern the folding of protein chains. *Science* 1973; 181:223–230.

37. Goldberg AL. Protein degradation and protection against misfolded or damaged proteins. *Nature* 2003; 426:895–899.
38. Macario AJL, Conway de Macario E. Sick chaperones, cellular stress, and disease. *N Engl J Med* 2005; 353:1489–1501.
39. Lindquist S. The heat-shock response. *Annu Rev Biochem* 1986; 55:1151–1191.
40. Storti RV, Scott MP, Rich A, Pardue ML. Translational control of protein synthesis in response to heat shock in D. *melanogaster* cells. *Cell* 1980; 22:825–834.
41. Lindquist S. Regulation of protein synthesis during heat shock. *Nature* 1981; 293:311–314.
42. Bienz M, Gurdon JB. The heat-shock response in *Xenopus* oocytes is controlled at the translational level. *Cell* 1982; 29:811–819.
43. Lindquist S. Translational efficiency of heat-induced messages in *Drosophila melanogaster* cells. *J Mol Biol* 1980; 137:151–158.
44. Landry J, Bernier D, Chrétien P, Nicole LM, Tanguay RM, Marceau N. Synthesis and degradation of heat shock proteins during development and decay of thermotolerance. *Cancer Res* 1982; 42:2457–2461.
45. Li GC, Werb Z. Correlation between synthesis of heat shock proteins and development of thermotolerance in Chinese hamster fibroblasts. *Proc Natl Acad Sci USA* 1982; 79:3218–3222.
46. Subjeck JR, Sciandra JJ, Johnson RJ. Heat shock proteins and thermotolerance: a comparison of induction kinetics. *Br J Radiol* 1982; 55:579–584.
47. Theodorakis NG, Morimoto RI. Posttranscriptional regulation of hsp70 expression in human cells: effects of heat shock, inhibition of protein synthesis, and adenovirus infection on translation and mRNA stability. *Mol Cell Biol* 1987; 7:4357–4368.
48. Li D, Duncan RF. Transient acquired thermotolerance in Drosophila, correlated with rapid degradation of Hsp70 during recovery. *Eur J Biochem* 1995; 231:454–465.
49. Mao RF, Rubio V, Chen H, Bai L, Mansour OC, Shi ZZ. OLA1 protects cells in heat shock by stabilizing HSP70. *Cell Death Dis* 2013; 4:e491.
50. Gerner C, Vejda S, Gelbmann D, et al. Concomitant determination of absolute values of cellular protein amounts, synthesis rates, and turnover rates by quantitative proteome profiling. *Mol Cell Proteomics* 2002; 1:528–537.
51. Snoeckx LH, Cornelussen RN, Van Nieuwenhoven FA, Reneman RS, Van Der Vusse GJ. Heat shock proteins and cardiovascular pathophysiology. *Physiol Rev* 2001; 81:1461–1497.
52. Xu Q. Role of heat shock proteins in atherosclerosis. *Arterioscler Thromb Vasc Biol* 2002; 22:1547–1559.
53. Xu Q, Metzler B, Jahangiri M, Mandal K. Molecular chaperones and heat shock proteins in atherosclerosis. *Am J Physiol Heart Circ Physiol* 2012; 302:H506–H514.
54. Currie RW, Karmazyn M, Kloc M, Mailer K. Heat-shock response is associated with enhanced postischemic ventricular recovery. *Circ Res* 1988; 63:543–549.
55. Donnelly TJ, Sievers RE, Vissern FL, Welch WJ, Wolfe CL. Heat shock protein induction in rat hearts: a role for improved myocardial salvage after ischemia and reperfusion? *Circulation* 1992; 85:769–778.
56. Hundt W, O'Connell-Rodwell CE, Bednarski MD, Steinbach S, Guccione S. In vitro effect of focused ultrasound or thermal stress on HSP70 expression and cell viability in three tumor cell lines. *Acad Radiol* 2007; 14:859–870.
57. Liu HL, Hsieh HY, Lu LA, Kang CW, Wu MF, Lin CY. Low-pressure pulsed focused ultrasound with microbubbles promotes an anticancer immunological response. *J Transl Med* 2012; 10:221.
58. Kruse DE, Mackanos MA, O'Connell-Rodwell CE, Contag CH, Ferrara KW. Short-duration-focused ultrasound stimulation of Hsp70 expression in vivo. *Phys Med Biol* 2008; 53:3641–3660.
59. Wu F, Wang ZB, Cao YD, et al. Expression of tumor antigens and heat-shock protein 70 in breast cancer cells after high-intensity focused ultrasound ablation. *Ann Surg Oncol* 2007; 14:1237–1242.
60. O'Brien WD Jr, Deng CX, Harris GR, et al. The risk of exposure to diagnostic ultrasound in postnatal subjects: thermal effects. *J Ultrasound Med* 2008; 27:517–535.
61. Liu GJ, Moriyasu F, Hirokawa T, Rexiati M, Yamada M, Imai Y. Expression of heat shock protein 70 in rabbit liver after contrast-enhanced ultrasound and radiofrequency ablation. *Ultrasound Med Biol* 2010; 36:78–85.
62. Sonne C, Xie F, Lof J, et al. Differences in Definity and Optison microbubble destruction rates at a similar mechanical index with different real-time perfusion systems. *J Am Soc Echocardiogr* 2003; 16:1178–1185.
63. Li P, Armstrong WF, Miller DL. Impact of myocardial contrast echocardiography on vascular permeability: comparison of three different contrast agents. *Ultrasound Med Biol* 2004; 30:83–91.
64. Locke M, Nussbaum E. Continuous and pulsed ultrasound do not increase heat shock protein 72 content. *Ultrasound Med Biol* 2001; 27:1413–1419.
65. Nussbaum EL, Locke M. Heat shock protein expression in rat skeletal muscle after repeated applications of pulsed and continuous ultrasound. *Arch Phys Med Rehabil* 2007; 88:785–790.
66. American Institute of Ultrasound in Medicine. Section 4—bioeffects in tissues with gas bodies. *J Ultrasound Med* 2000; 19:97–108, 154–168.
67. Miller DL, Averkiou MA, Brayman AA, et al. Bioeffects considerations for diagnostic ultrasound contrast agents. *J Ultrasound Med* 2008; 27:611–616.
68. Udelsman R, Blake MJ, Stagg CA, Li DG, Putney DJ, Holbrook NJ. Vascular heat shock protein expression in response to stress: endocrine and autonomic regulation of this age-dependent response. *J Clin Invest* 1993; 91:465–473.
69. Snoeckx LH, Contard F, Samuel JL, Marotte F, Rappaport L. Expression and cellular distribution of heat-shock and nuclear oncogene proteins in rat hearts. *Am J Physiol* 1991; 261:H1443–H1451.
70. Gil AG, Silván G, Illera M, Illera JC. The effects of anesthesia on the clinical chemistry of New Zealand White rabbits. *J Am Assoc Lab Anim Sci* 2004; 43:25–29.
71. Gil AG, Silván G, Villa A, Millán P, Martínez-Fernández L, Illera JC. Serum biochemical response to inhalant anesthetics in New Zealand White rabbits. *J Am Assoc Lab Anim Sci* 2010; 49:52–56.
72. Constans J, Conri C. Circulating markers of endothelial function in cardiovascular disease. *Clin Chim Acta* 2006; 368:33–47.
73. Spiel AO, Gilbert JC, Jilma B. von Willebrand factor in cardiovascular disease: focus on acute coronary syndromes. *Circulation* 2008; 117:1449–1459.